In Silico Study of Entry Inhibitor from Moringa oleifera Bioactive Compounds against SARS-CoV-2 Infection

Nala Mawaddani[1], Ekris Sutiyanti[2], Muhammad Hermawan Widyananda[1], Viol Dhea Kharisma[3], Dora Dayu Rahma Turista[4], Muhammad Badrut Tamam[5], Vikash Jakhmola[6], Syamsurizal[7,8], Bayu Ramadhani Fajri[7,9], Muhammad Raffi Ghifari[7,10], Muhammad Thoriq Albari[7,10], Muhammad Arya Ghifari[7,10], Amalia Putri Lubis[7,11], Dony Novaliendry[7,12], Dwi Hilda Putri[7,8], Fadhilah Fitri[7,13], Devni Prima Sari[7,14], Alexander Patera Nugraha[15], ANM Ansori[16], Maksim Rebezov[17,18,19], Rahadian Zainul[7,11,*]

[1]Department of Biology, Faculty of Mathematics and Natural Sciences, Universitas Brawijaya, Malang, INDONESIA.

[2]Department of Tropical Biology, Faculty of Biology, Universitas Gadjah Mada, Yogyakarta, INDONESIA.

[3]Division of Molecular Biology and Genetics, Generasi Biologi Indonesia Foundation, Gresik, INDONESIA.

[4]Biology Education Department, Faculty of Teacher Training and Education, Mulawarman University, Samarinda, INDONESIA.

[5]Department of Biology, Faculty of Sciences and Technology, Universitas Muhammadiyah Lamongan, Lamongan, INDONESIA.

[6]Uttaranchal Institute of Pharmaceutical Sciences, Uttaranchal University, Dehradun, INDIA.

[7]Center for Advanced Material Processing, Artificial Intelligence, and Biophysics Informatics (CAMP-BIOTICS), Universitas Negeri Padang, Padang, INDONESIA.

[8]Department of Biology, Faculty of Mathematics and Natural Sciences Universitas Negeri Padang, Padang, INDONESIA.

[9]Information Technology, Dapartement of Electronic, Faculty of Engineering, Universitas Negeri Padang, Padang, INDONESIA.

[10]Department of Information Technology, Faculty of Computer Sciences, Universitas Brawijaya, Malang, INDONESIA.

[11]Department of Chemistry, Faculty of Mathematics and Natural Sciences Universitas Negeri Padang, Padang, INDONESIA.

[12]Program Study Informatics, Faculty of Engineering, Universitas Negeri Padang, Padang, INDONESIA.

[13]Department of Statistics, Faculty of Mathematics and Natural Sciences Universitas Negeri Padang, Padang, INDONESIA.

[14]Department of Mathematics, Faculty of Mathematics and Natural Sciences, Universitas Negeri Padang, Padang, INDONESIA.

[15]Department of Orthodontics, Faculty of Dental Medicine, Universitas Airlangga, Surabaya, INDONESIA.

[16]Professor Nidom Foundation, Surabaya, INDONESIA.

[17]Department of Scientific Research, Russian State Agrarian University - Moscow Timiryazev Agricultural Academy, Moscow, RUSSIAN FEDERATION

[18]Faculty of Biotechnology and Food Engineering, Ural State Agrarian University, Yekaterinburg, RUSSIAN FEDERATION

[19]Department of Scientific Research, K.G. Razumovsky Moscow State University of Technologies and Management (The First Cossack University), Moscow, RUSSIAN FEDERATION

Correspondence

Rahadian Zainul

Center for Advanced Material Processing, Artificial Intelligence, and Biophysic Informatics (CAMP-BIOTICS), Department of Biology, Faculty of Mathematics and Natural Sciences Universitas Negeri Padang, Padang, INDONESIA.

E-mail: rahadianzmsiphd@fmipa.unp.ac.id

ABSTRACT

The aim of this study is to screen the content of bioactive compounds of *Moringa oleifera* and to identify its potential as an antiviral against COVID 19 through an entry inhibitor mechanism using bioinformatics tools. The sample was obtained from PubChem database. Amino acis sequences were obtained from the NCBI. Protein modeling is made through the SWISSMODEL site. The target proteins for this study were SARS-CoV-2 M^{pro} and RdRp. The protein-inhibitory interaction of the drug from *M. oleifera* bioactive compounds to SARS-CoV-2 was predicted by molecular docking with PyRx software. The result shows that *M. oleifera* was a potential antiviral candidate for SARS-CoV-2 with an entry inhibitor mechanism through a compound, especially quercetin. The RFMS value of both interactions between M^{pro} and quercetion and RdRp with quercetin were not higher than 1.05. This result still needed further research to prove this prediction.

Key words: COVID-19, M^{pro}, RdRp, *Moringa oleifera*, Active site.

INTRODUCTION

Coronavirus (CoV) also known as COVID 19, has spread worldwide in December 2019 and became a pandemic in January 2022.[1,2] WHO declared in March 2020 that this pandemic transmission is a person to person. The case of COVID 19 has enlarged widely to 213 countries and it caused more than 270 million infections over 5 million cases and those numbers still rising.[3] WHO confirmed the symptoms of COVID 19 were fever, dry cough, respiratory disorders, and olfactory and taste disorders.[4-7]

The human coronavirus (HCoV) was positive-stranded RNA virus. There were 2 types of protein of HCoV structural and non-structural protein that have different characteristics. The structural protein has characteristics including envelope, matrix, nucleocapsid, and spike. Besides, the non-structural protein has RNA-dependent RNA polymerase (RdRp).[8] RdRp has an important role in the HCoV life cycle and also became the main target factor for COVID 19 therapeutics. According to the Genome report, SARS-CoV-2depends on the viral protein function of the main protease (M^{pro}).[9] M^{pro} has the main role in SARS-CoV-2 transcription and replication.[10,11] Hence, M^{pro} and RdRp were the best candidates for designing antiviral drugs to find therapeutics agents against SARS-CoV-2.

Moringa oleifera is also known as the "miracle tree" because it has abundant benefits.[12-14] There were bioactive compounds obtained from *M. Oleifera* including Aurantiamide acid, Anthraquinone, Apigenin, Benzyl isothiocyanate, Chrysin, Dibutyl phthalate, Ellagic acid, Hydroxychloroquinone, Isorhamnetin, Kaemferol, Myrcetin, Pterygospermin, Quercetin, Rutin, and β-amyrin which has an antiviral potential compounds against COVID 19 by inhibiting M^{pro} and RdRp activity.[15-18] Besides all the compounds above, Oleic acid was most found at around 84% in *M. Oleifera*.[19] *M. oleifera* was the most appropriate candidate for an antiviral agent against SARS-CoV-2. The aim of this study was to screen bioactive compounds of *Moringa oleifera* and to identify the antiviral potential compounds toward SARS-CoV-2 through an entry inhibitor mechanism.

METHODS

Data mining of sample

The bioactive compounds of *M. oleifera* which consist of anthraquinone, apigenin, aurantiamide acetate, benzyl isothiocyanate, chlorogenic acid, chrysin, dibutyl phthalate, ellagic acid, hesperidin, isorhoifolin, myricetin, pterygospermin, quercetin, rutin, and vitex. The bioactive compounds of *M. oleifera* were retrieved format from PubChem database (https://pubchem.ncbi.nlm.nih.gov/) in sdf format.[20]

Protein modeling

The structure of M^{pro} and RdRp as the target proteins which were not available in the RCSB PDB database was modeled based on their amino acid sequence. The NCBI (https://www.ncbi.nlm.nih.gov/) database was used to retrieve sequences of amino acids with fasta format. Furthermore, protein modeling is made through the SWISSMODEL site (https://swissmodel.expasy.org/). The selection of protein models was selected from several parameters such as QMQE value, QMEAN value, coverage value, local quality value, and comparison plot. In addition, the protein

structure also reviewed the Ramachandran Plot value according to favored, allowed, and outlier regions.[21]

Bioactivity and drug likeness prediction

Bioactivity of active compounds were predicted according to probability values (Pa) through PASS online site (http://way2drug.com/passonline/). To be an effective drug, potential active compounds must be able to reach the target in the body. There were several characteristics that a drug must possess in order to reach the target in the body to be selected as a drug potential. The characteristics reviewed include molecular mass, TPSA value, solubility in lipids, and others. There were several parameters to be reviewed in drug-likeness, named Lipinksi, Ghose, Veber, Egan, and Muegge Parameter. Prediction of drug-likeness could be done through the SWISS ADME (http://www.swissadme.ch) website. Active compounds that fulfill five parameters will be selected.[8,22,23]

Ligand and protein preparation

The minimization energy process of the ligand was prepared with PyRx software. Ligand preparation aimed to increase flexibility and change the sdf format to pdb. Ligand preparation also to minimize the binding affinity. The target protein in this paper was the M^{pro} and RdRp. Sterilization of the target protein from water and contaminant ligands was carried out by Discovery Studio software to increase the optimization of binding energy.[20,24,25]

Molecular docking and dynamic simulation

Molecular docking with the PyRx software was performed to predict the interaction of protein inhibition on SARS-COV 2 by active compounds from *M. oleifera*.[26] Molecular docking of the M^{pro} target was done by blind docking. On the other hand, molecular docking of the RdRp target was done by specific docking at its catalytic sites: Gly-616, Trp-617, Asp-618, Tyr-619, Leu-758, Ser-759, Asp-760, Asp-761, Ala-762, Lys-798, Tys-799, Trp-800, Glu-811, Phe-812, Cys-813, and Ser-814.[27] The validation of the docking results were carried out with a dynamic molecular test by using CABS-flex 2.0. At this stage, the Fluctuation Plot tab on CABS-flex 2.0 showed the residue fluctuation profile due to the RMSF value for protein target.[28]

Docking visualization

The analysis of the docking results was reviewed based on the 2D and 3D forms. Visualization of 2D docking results was done by Discovery Studio software. Moreover, the 3D visualization was carried out with PyMOL. Types of interactions and chemical bonds formed were analyzed using the Discovery Studio software.[26,29]

RESULT AND DISCUSSION

Bioactivity and drug-like molecule potential of the bioactive compounds in the *M. oleifera*

The data of bioactive compounds found in *Moringa oleifera*, such as anthraquinone (CID 6780), apigenin (CID 5280443), aurantiamide acetate (CID 124319), benzyl isothiocyanate (CID 2346), chlorogenic acid (CID 1794427), chrysin (CID 5281607), dibutyl phthalate (CID 3026), ellagic acid (CID 5281855), hesperidin (CID 10621), isorhoifolin (CID 9851181), myricetin (CID 5281672), pterygospermin (CID 72201063), quercetin (CID 5280343), rutin (CID 5280805) and vitexin (CID 5280441) were acquired from the PubChem database (https://pubchem.ncbi.nlm.nih.gov/). Biological activity potential of all compounds were evaluated with PASS online site based on their chemical structure. The estimated value of probability was shown by probability activity value (Pa) and probability inactivity (Pi) from 0.000 to 1.000. High value of Pa means higher bioactivity.[30] The result of bioactivity prediction of bioactive compounds of *M. oleifera* (Table 1).

Drug-likeness analysis aimed to identify molecules considered to be drugs built upon their physicochemical properties. The properties approaches aimed to measure drug likeness consist of octanol–water partition coefficient (ALOGP), number of H-bond acceptors (HBAs), number of H-bond donors (HBDs), molecular weight (MW), molecular polar surface area (PSA), number of aromatic rings (AROMs), number of structural alerts (ALERTS) and number of rotatable bonds (ROTBs).[31] Based on these properties, there are several relevant drug likeness rules such those proposed by Lipinski, Ghose, Veber, Eggan and Muegge. These rules suggest the compound as a drug based on their physicochemical properties. The Lipophilicity (log $P_{o/w}$) is the partition coefficient between water and n-octanol. Water solubility is the value of a drug's ability for oral targeting. SwissADME provides the number of violations in every rule.[30] The drug likeness prediction of bioactive compounds of *M. oleifera* (Table 2) and drug likeness parameter of bioactive compounds of *M. oleifera* (Table 3).

The Binding activity ability and molecules interaction of the bioactive compounds in the *M. oleifera* and target protein

The bioactive compounds of M. *oleifera* and target protein generate interactions and binding activity. Based on the result of the study showed two different proteins targets were M^{pro} and RdRp which interacted with bioactive compounds of *M. oleifera*. The lowest binding affinity value of M^{pro} and RdRp interactions were M^{pro} – Apigenin -7.8 kcal/mol, M^{pro} – Quercetin -7.3 kcal/mol, RdRp – Quercetin -6.9 kcal/mol, RdRp – Pterygospermin -6.6 kcal/mol (table 4 & 5). Respectively, implying that M^{pro} more easily binds to Apigenin than Quercetin and RdRp binds strongly to Quercetin than Pterygospermin. There are different amino acid residues of each receptor bound to the ligand based on the visualization by Discovery Studio. The 3D complex of the interactions formed is visualized and can be clearly distinguished between the receptor and its ligand (figure 1 & 2). The types of bonds and variations in the binding positions formed from the complexes were demonstrated in the 2D visualization performed by Discovery Studio (figure 1 & 2). In addition, the results of 2D visualization by Discovery Studio showed different colors in different interactions. The colors indicate the type of bonds formed from the complex. The amino acid residues that bind to the ligand can be seen from the interaction points, distances, chemistry bonds, and type through the discovery studio application (figure 1 & 2; table 4 & 5).

Based on the docking Discovery studio visualization showed that there were several ligands which binds to both M^{pro} and RdRp active sites. Apigenin (glu-166, cys-145), Chrysin (glu-166, cys-145), and quercetin (cys 145) binds to the active site of M^{pro}, while Anthraquinone (glu-811, trp-800, lys-798), Apigenin (ser-814, cis-813, asp-760, asp-761), Chrysin (asp-761, lys-798, glu-811), Dibutyl phthalate (asp-761, ser-814, cys-813, trp-800), Pterygospermin (glu-811, lys-798, asp-618), and Quercetin (glu-811, asp-760, asp-761, tyr-619) which binds to active site of RdRp SARS-CoV-2. The interaction of M^{pro} and Apigenin generates a conventional hydrogen bond and 2 Pi-sulfur bonds. M^{pro} and Chrysin generates Pi-Donor hydrogen bond and 2 Pi-sulfur bonds. M^{pro} and Quercetin generate Pi-alkyl bond. The interaction RdRp and anthraquinone generates a conventional hydrogen bond, 2 Pi-alkyl bonds, and 2 Pi-anion bonds. RdRp and Apigenin generate 2 conventional hydrogen bonds and 3 Pi-anion bonds. RdRp and Chrysin generate a conventional hydrogen bond, 2 Pi-anion bonds, and a Pi-alkyl bond. RdRp Dibutyl phthalate generates 3 conventional hydrogen bonds, a Pi-anion bond, and a Pi-alkyl bond. RdRp and Pterygospermin generate a conventional hydrogen bond, a Pi-anion bond, and a Pi-alkyl bond. RdRp and Quercetin generate 5 conventional hydrogen bonds (table 4 & 5).

M^{pro} was a cysteine protease that moderates the maturation cleavage of polyprotein in virus replication and also plays a crucial role in the

Table 1: Bioactivity prediction result.

Compound	Antiviral	Non-Steroidal Anti Inflammatory Agent	Anti-Inflammatory	Viral Entry Inhibitor	3C-like protease (Human coronavirus) inhibitor	Viral fusion inhibitor
Rutin	0.263	0.518	0.728			
Isorhoifolin	0.235		0.705			
Quercetin	0.262			0.257		
Hesperidin	0.193					
Ellagic acid	0.322		0.749	0.265	0.241	
Aurantiamide acetate	0.217		0.249	0.209	0,341	
Benzyl isothiocyanate				0,219	0,267	0,011
Dibutyl phthalate			0,497	0,215	0,293	
Pterygospermin				0,227	0,251	0,010
Apigenin	0,209		0,644	0,243	0,267	
Chrysin	0,212		0,637	0,242	0,273	
Myricetin	0,334		0,720	0,272	0,197	
Chlorogenic acid	0,303		0,598			
Vitexin	0,360		0,606			
Anthraquinone		0.295	0.410	0.267	0.326	

Table 2: Drug likeness prediction result.

Compound	MW (g/mol)	MiLogP	HBD	HBA	TPSA (Å²)	Bioavailability
Rutin	610.52	-3.89	16	10	269.43	0.17
Isorhoifolin	578.52	-2.96	8	14	228.97	0.17
Quercetin	302.24	-0.56	5	7	131.36	0.55
Hesperidin	610.56	-3.04	8	15	234.29	0.17
Ellagic acid	302.19	0.14	4	8	141.34	0.55
Aurantiamide acetate	444.52	3.41	2	4	84.50	0.55
Benzyl isothiocyanate	149.21	3.28	0	1	44.45	0.55
Dibutyl phthalate	278.34	3.43	0	4	52.60	0.55
Pterygospermin	406.52	2.68	0	2	89.12	0.55
Apigenin	270.24	0.52	3	5	90.90	0.55
Chrysin	254.24	1.08	2	4	70.67	0.55
Myricetin	318.24	-1.08	6	8	151.59	0.55
Chlorogenic acid	354.31	-1.05	6	9	164.75	0.11
Vitexin	432.38	-2.02	7	10	181.05	0.55
Anthraquinone	208.21	1.86	0	2	34.14	0.55

Table 3: Drug likeness parameter.

Compound	Drug Likeness Parameter Violation				
	Lipinski	Ghose	Veber	Egan	Muegge
Rutin	3	4	1	1	4
Isorhoifolin	3	4	1	1	3
Quercetin	0	0	0	0	0
Hesperidin	3	4	1	1	4
Ellagic acid	0	0	1	1	0
Aurantiamide acetate	0	0	1	0	0
Benzyl isothiocyanate	0	2	0	0	1
Dibutyl phthalate	0	0	0	0	0
Pterygospermin	0	0	0	0	0
Apigenin	0	0	0	0	0
Chrysin	0	0	0	0	0
Myricetin	1	0	1	1	2
Chlorogenic acid	1	1	1	1	2
Vitexin	1	0	1	1	2
Anthraquinone	0	0	0	0	0

Table 4: Molecular docking result of compounds from *Moringa oleifera* againts M^pro.

Interaction	Binding affinity (kcal/mol)	Interaction point	Distance (Å)	Chemistry bond	Types
M^pro – Anthraquinone	-7.0	A:GLN110:NE2 - :LIG1:O	3.16225	Hydrogen Bond	Conventional Hydrogen Bond
		A:SER158:OG - :LIG1:O	3.21938	Hydrogen Bond	Conventional Hydrogen Bond
		A:ASN151:ND2 - :LIG1	4.06044	Hydrogen Bond	Pi-Donor Hydrogen Bond
		A:ILE106:CG2 - :LIG1	3.90218	Hydrophobic	Pi-Sigma
		:LIG1 – A:PHE294	5.29534	Hydrophobic	Pi-Pi T-shaped
		:LIG1 – A:VAL104	5.14081	Hydrophobic	Pi-Alkyl
M^pro - Apigenin	-7.8	:LIG:H – A:TYR54:OH	2.28149	Hydrogen Bond	Conventional Hydrogen Bond
		:LIG:H – A:ASP187:O	2.67618	Hydrogen Bond	Conventional Hydrogen Bond
		:LIG:H – :LIG1:O	2.39102	Hydrogen Bond	Conventional Hydrogen Bond
		:LIG:H – A:LEU141:O	2.0859	Hydrogen Bond	Conventional Hydrogen Bond
		:LIG:H – A:SER144:O	2.50024	Hydrogen Bond	Conventional Hydrogen Bond
		A:GLU166:N - :LIG1	4.06547	Hydrogen Bond	Conventional Hydrogen Bond
		A:CYS145:SG - :LIG1	5.57509	Other	Pi-Sulfur
		A:CYS145:SG - :LIG1	5.14695	Other	Pi-Sulfur
		:LIG1 – A:MET49	4.69304	Hydrophobic	Pi-Alkyl
M^pro - Chrysin	-7.2	:LIG1:H – A:LEU141:O	2.14346	Hydrogen Bond	Conventional Hydrogen Bond
		:LIG1:H – A:SER144:OG	2.55404	Hydrogen Bond	Conventional Hydrogen Bond
		A:GLU166:N - :LIG1	4.03044	Hydrogen Bond	Pi-Donor Hydrogen Bond
		A:CYS145:SG - :LIG1	5.55701	Other	Pi-Sulfur
		A:CYS145:SG - :LIG1	5.12793	Other	Pi-Sulfur
		:LIG1 – A:MET49	4.71637	Hydrophobic	Pi-Alkyl
M^pro – Dibutyl Phthalate	-5.3	A:GLN110:NE2 – LIG1:O	3.25421	Hydrogen Bond	Conventional Hydrogen Bond
		A:ASN151:ND2 - :LIG1:O	2.96662	Hydrogen Bond	Conventional Hydrogen Bond
		A:ASN151:ND2 - :LIG1:O	3.01994	Hydrogen Bond	Conventional Hydrogen Bond
		:LIG1:C – A:SER158:OG	3.64073	Hydrogen Bond	Carbon Hydrogen Bond
		A:SER158:CB - :LIG1:O	3.57752	Hydrogen Bond	Carbon Hydrogen Bond
		:LIG1:C - :LIG1	3.71143	Hydrophobic	Pi-Sigma
		A:ILE106:CG2 - :LIG1	3.65094	Hydrophobic	Pi-Sigma
		:LIG1 A:VAL104	5.26739	Hydrophobic	Pi-Alkyl
		A:PHE294 - :LIG1	3.99071	Hydrophobic	Pi-Alkyl
M^pro - Pterygospermin	-6.3	:LIG1:S – A:TYR237:O	3.6789	Hydrogen Bond	Conventional Hydrogen Bond
		A:LYS137:NZ - :LIG1:S	3.68971	Hydrogen Bond	Conventional Hydrogen Bond
		:LIG1:C – A:THR199:OG1	3.53423	Hydrogen Bond	Carbon Hydrogen Bond
		:LIG1:C – A:TYR237:O	3.44575	Hydrogen Bond	Carbon Hydrogen Bond
		:LIG1:C – A:ASP197:OD2	3.77204	Hydrogen Bond	Carbon Hydrogen Bond
		A:ASP289:OD1 - :LIG1	4.12393	Electrostatic	Pi-Anion
		A:TYR239:OH - :LIG1	3.52753	Hydrogen Bond	Pi-Donor Hydrogen Bond
		:LIG1:S – A:TYR237	5.84567	Other	Pi-Sulfur
		:LIG1 – A:LEU287	4.96378	Hydrophobic	Pi-Alkyl
M^pro - Quercetin	-7.3	:LIG:H – A:LEU141:O	2.17236	Hydrogen Bond	Conventional Hydrogen Bond
		:LIG:H – A:SER144:OG	2.29642	Hydrogen Bond	Conventional Hydrogen Bond
		:LIG:H – A:MET165:SD	2.67346	Hydrogen Bond	Conventional Hydrogen Bond
		A:SER144:OG - :LIG1:O	3.11122	Hydrogen Bond	Conventional Hydrogen Bond
		A:GLN189:CA - :LIG1	3.35174	Hydrogen Bond	Carbon Hydrogen Bond
		A:MET165:SD - :LIG1	5.3728	Other	Pi-Sulfur
		:LIG1 – A:CYS145	4.88012	Hydrophobic	Pi-Alkyl

Table 5: Molecular docking result of compounds from Moringa oleifera againts RdRp.

| Interaction	Binding afinity (kcal/mol)	Interaction point	Distance (Å)	Chemistry bond	Types
		A:TRP800:NE1 - :LIG1:O	3.17196	Hydrogen Bond	Conventional Hydrogen Bond
		A:GLU811:OE1 - :LIG1	4.11437	Electrostatic	Pi-Anion
RdRp – Anthraquinone	-5.7	A:GLU811:OE1 - :LIG1	3.6791	Electrostatic	Pi-Anion
		LIG1 – A:LYS798	5.24834	Hydrophobic	Pi-Alkyl
		:LIG1 – A:LYS798	4.93519	Hydrophobic	Pi-Alkyl
		A:CYS813:N - :LIG1:O	3.24885	Hydrogen Bond	Conventional Hydrogen Bond
		A:SER814:N - :LIG1:O	3.02667	Hydrogen Bond	Conventional Hydrogen Bond
RdRp - Apigenin	-6.4	A:ASP760:OD1 - :LIG1	4.40583	Electrostatic	Pi-Anion
		A:ASP761:OD1 - :LIG1	3.90294	Electrostatic	Pi-Anion
		A:ASP761:OD1 - :LIG1	3.23159	Electrostatic	Pi-Anion
		:LIG1:H – A:ASP761:OD2	2.80245	Hydrogen Bond	Conventional Hydrogen Bond
RdRp - Chrysin	-6.4	A:GLU811:OE1 - :LIG1	3.5163	Electrostatic	Pi-Anion
		A:GLU811:OE1 - :LIG1	4.50699	Electrostatic	Pi-Anion
		:LIG1 – A:LYS798	3.73501	Hydrophobic	Pi-Alkyl
		A:TRP800:NE1 - :LIG1:O	3.36979	Hydrogen Bond	Conventional Hydrogen Bond
		A:CYS813:N - :LIG1:O	3.17805	Hydrogen Bond	Conventional Hydrogen Bond
		A:SER814:N - :LIG1:O	2. 85424	Hydrogen Bond	Conventional Hydrogen Bond
RdRp – Dibutyl Phthalate	-4.4	A:ASP761:OD1 - :LIG1	3.2988	Electrostatic	Pi-Anion
		:LIG1:C - :LIG1	3.8863	Hydrophobic	Pi-Sigma
		:LIG1 – A:LYS798	4.3898	Hydrophobic	Pi-Alkyl
		:LIG1:S – A:GLU811:O	3.68091	Hydrogen Bond	Conventional Hydrogen Bond
RdRp - Pterygospermin	-6.6	A:ASP618:OD1 - :LIG1	4.34769	Electrostatic	Pi-Anion
		:LIG1 – A:LYS798	4.34806	Hydrophobic	Pi-Alkyl
		:LIG1:H – A:GLU811:O	1.93037	Hydrogen Bond	Conventional Hydrogen Bond
		:LIG1:H – A:ASP760:O	2.46817	Hydrogen Bond	Conventional Hydrogen Bond
RdRp – Quercetin	-6.9	:LIG1:H – A:ASP761:OD1	2.64803	Hydrogen Bond	Conventional Hydrogen Bond
		:LIG1:H – A:ASP760:OD1	2.5649	Hydrogen Bond	Conventional Hydrogen Bond
		A:TYR619:N - :LIG1:O	3.19529	Hydrogen Bond	Conventional Hydrogen Bond
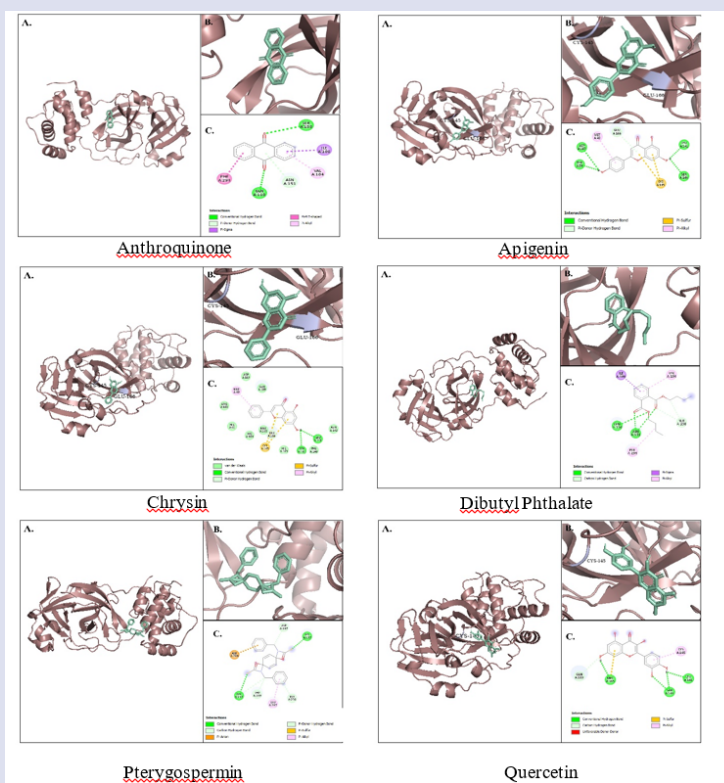
Figure 1: Protein interaction conserved region amino acid residues of Mpro. (A) 3D structure of protein interactions Mpro with bioactive compounds in *Moringa oleifera*, (B) Magnification view 3D structure of protein interactions Mpro with bioactive compounds in *Moringa oleifera*, (C) 2D structure of protein interactions Mpro with bioactive compounds in *Moringa oleifera*.
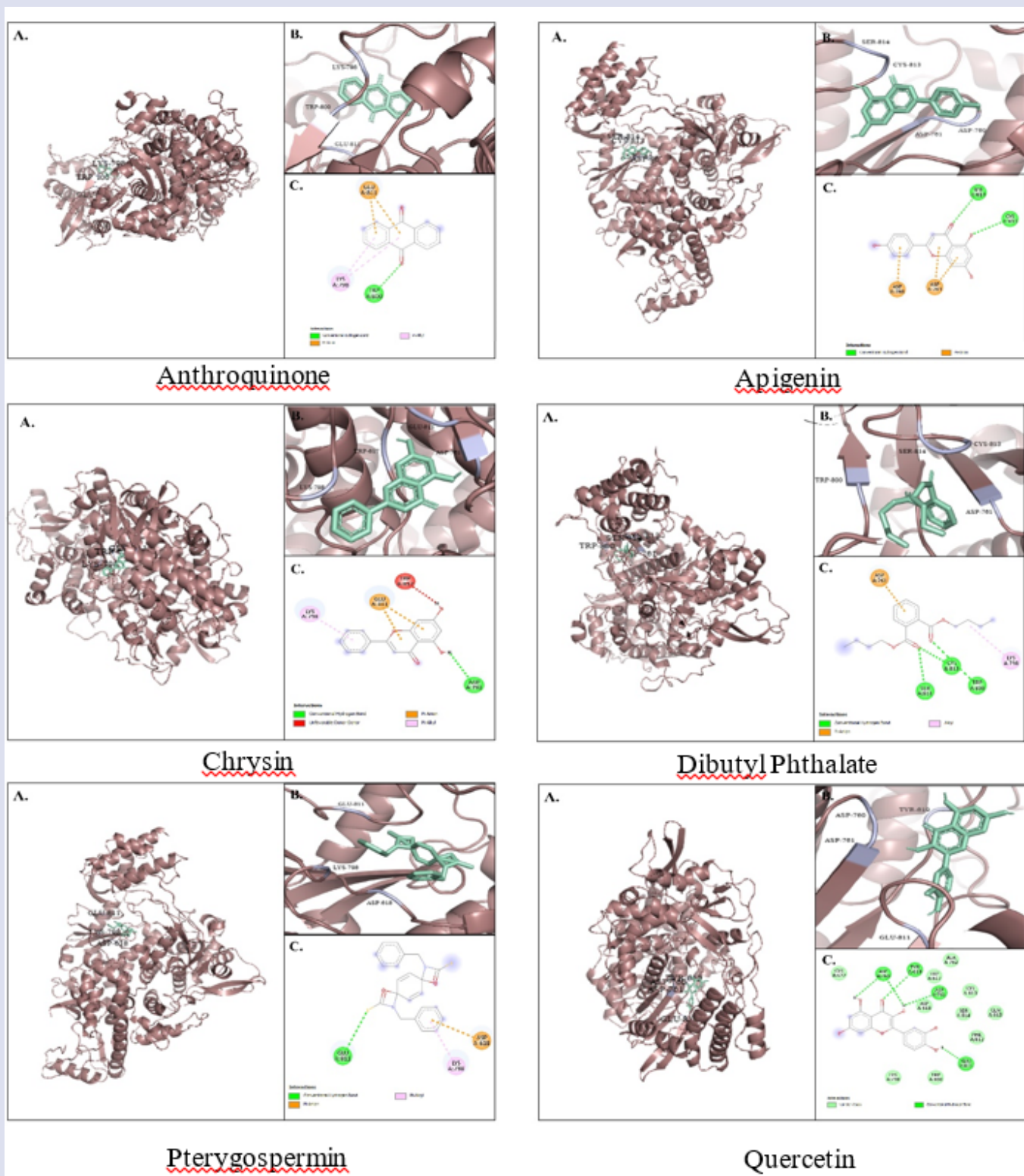
Figure 2: Protein interaction conserved region amino acid residues of RdRp. (A) 3D structure of protein interactions RdRp with bioactive compounds in *Moringa oleifera*, (B) Magnification view 3D structure of protein interactions RdRp with bioactive compounds in *Moringa oleifera*, (C) 2D structure of protein interactions RdRp with bioactive compounds in *Moringa oleifera*.
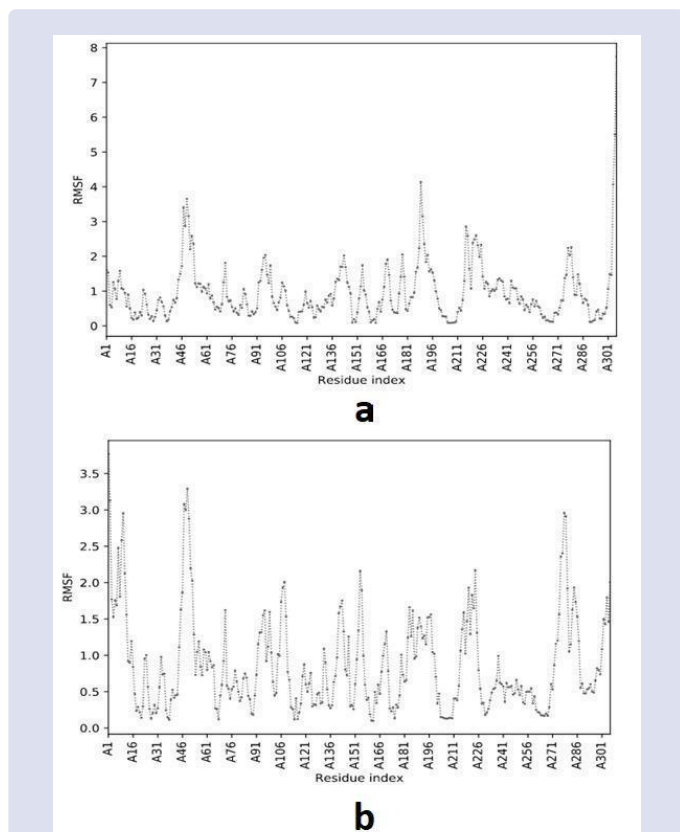
Figure 3: Visualization of molecular dynamic simulation results. (A) RMSF of Mpro-Apigenin, (B) RMSF of Mpro-Quercetin.
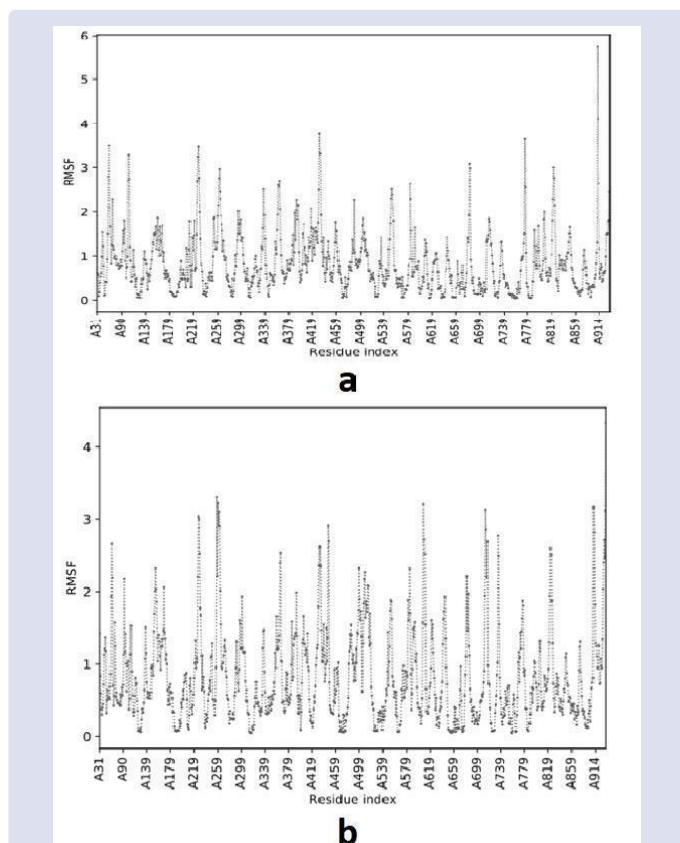

Figure 4: Visualization of molecular dynamic simulation results. (A) RMSF of RdRp-Pterygospermin, (B) RMSF of RdRp-Quercetin.

virus transcription of the life cycle.[32] Cys-145, Glu-166, and His-163 were the most attractive residue of SARS-CoV-2 Mpro to form hydrogen bonds.[32-34] The location of Mpro substrate-binding site was between domains I and II, which was Cys-145 and His-41 were catalytic activity site.[32-35] In line with this study which Mpro binds to apigenin, chrysin, and quercetin in Cys-145. Besides Mpro, RdRp also plays a pivotal role in the viral life cycle. The most reachable and conserved region in viral replication was RdRp, therefore it can be an effective target for antiviral drugs for SARS-CoV-2.[27,36,37] RdRp catalytic sites included Ala-762, Asp-618, Asp-761, Cys-813, Glu-811, Gly-616, Leu-758, Lys-798, Phe-812, Ser-760, Ser-814, Trp-617, Trp-800, Tyr-619, Tys-799.[27] In line with this study, RdRp binds to anthraquinone (Glu-811, Trp-800, Lys-798), Apigenin (Ser-814, Cys-813, Asp-760, Asp-761), Chrysin (Asp-761, Lys-798, Glu-811), Dibutyl phthalate (Asp-761, Ser-814, Cys-813, Trp-800), Pterygospermin (Glu-811, Lys-798, Asp-618) and Quercetin (Glu-811, Asp-760, Asp-760, Tyr-619).

A recent report has shown that remdesivir is able to inhibit replication of SARS-CoV-2 in *in vitro* and *in vivo* experiment.[38,39] Remdesivir is an adenosine analogue that inhibits SARS-CoV-2 RdRp.[32-40] Therefore, remdesivir can be used as a positive control in this study. According to the result docking simulations.[41] Based on the research showed that remdesivir probably binds to Mpro stronger than to RdRp.[32] The Mpro residues that form a hydrogen bond with remdesivir are His-163, Ser-144, and Leu-141, and non-bonded contacts are associated with Glu-166, Cys-145, Met-165, Gln-189, Arg-188, Asp-187, His-41, Met-49, Thr-26, Leu-27, Thr-45, and Thr25. In line with this study, the result shows that interaction Mpro - Apigenin has the lowest binding affinity value -7.8 kcal/mol with interaction point active site Glu-166 and Cys-145, and Mpro – Quercetin binding affinity value -7.3 kcal/mol with interaction point Cys-145. These results indicate that both apigenin, quercetin, and remdesivir bind to Glu-166 and Cys-145 of the active site of Mpro.[42] While the interaction residues between RdRp and remdesivir are 56 residues, 10 of those residues were involved in a catalytic activity such as Ala-558, Asp-684, Asp-760, Asp-761, Cys-813, Gly-559, Ser-682, Ser-759, and Ser-814.[43] In line with this study result shows that interaction RdRp to anthraquinone (Glu-811, Trp-800, Lys-798), Apigenin (Ser-814, Cys-813, Asp-760, Asp-761), Chrysin (Asp-761, Lys-798, Glu-811), Dibutyl phthalate (Asp-761, Ser-814, Cys-813, Trp-800), Pterygospermin (Glu-811, Lys-798, Asp-618) and Quercetin (Glu-811, Asp-760, Asp-760, Tyr-619). These results indicate that catalytic sites Asp-760, Asp-761, and Cys813 were found in the interaction of RdRp and remdesivir, apigenin, chrysin, dibutyl phthalate, pterygospermin, and quercetin.

Molecular dynamics simulation of *M. oleifera's* bioactive compounds with SARS-CoV-2 glycoprotein

Simulation parameters and a set of distance restraints used by CABS-flex. Molecular Dynamics (MD) simulations carried out to generate the best convergence between either CABS-flex simulation and protein fluctuation simulation in aqueous solution. MD was carried out by 10 nanoseconds in length. In addition, MD was derived by different force fields for globular protein.[28] MD aims to support molecular docking results. The root-mean-square fluctuation (RMSF) was a measure of the displacement of the position of the protein atom relative to the reference structure. RMSF analyzes the portions of structure that are fluctuating from their mean structure.[44] Figure 3 showed the information of flexibility of Mpro with its interaction with Apigenin and Quercetin, figure 4 showed the information of flexibility of RdRp with its interaction with Pterygospermin and Quercetin. Based on,[45] the RMFS average value of Mpro and Remdevisir is below 0.4. Meanwhile, based on the result of our molecular dynamics, the average of Mpro-Apigenin's RMFS value at the catalytic site is 1.24 nm and the average of Mpro-Quercetin's RMFS value at the catalytic site is 1.04 nm. It was a

few greater than the RMFS's value of Remdevisir. Based on,[46] the RMFS value of RdRp and Remdevisir in initial residues which were from first sequence of amino acid to 125th amino acid sequence, showed a relatively higher fluctuation value of 0.6–0.75 nm. Whereas, residues after 125th sequences showed stationary value of 0.4 nm. Meanwhile, according to the result of our molecular dynamics, the average of RdRp-Pterygospermin's RMFS value at the catalytic site is 0.5 nm and the average of RdRp-Quercetin's RMFS value at the catalytic site is 0.58 nm. It was a few greater than the RMFS's value of Remdevisir.

CONCLUSION

Our *in silico* studies suggest *M. oleifera* as a potential antiviral candidate for SARS-CoV-2 with an entry inhibitor mechanism through a compound, specifically quercetin. Quercetin shows the activity as antiviral against SARS-CoV-2 by bind to the both active sites of M^{pro} and RdRp of the SARS-CoV-2 with more negative binding affinity than the other compound, resulting in interactions between hydrogen bonds and hydrophobic bonds. Moreover, the RFMS value of the interaction between M^{pro} and quercetin and RdRp with quercetin were not higher than 1.05. Furthermore, experimental *in vitro* and *in vivo* studies both are necessary to prove this *in silico* predictions.

REFERENCES

1. Ansori AN, Kharisma VD, Parikesit AA, Dian FA, Probojati RT, Rebezov M, *et al*. Bioactive Compounds from Mangosteen (*Garcinia mangostana* L.) as an Antiviral Agent via Dual Inhibitor Mechanism against SARS-CoV- 2: An in Silico Approach. Pharmacogn J. 2022;14(1):85-90.

2. Ansori ANM, Kharisma VD, Fadholly A, Tacharina MR, Antonius Y, Parikesit AA. Severe Acute Respiratory Syndrome Coronavirus-2 Emergence and Its Treatment with Alternative Medicines: A Review. Res J Pharm Technol. 2021;14(10):5551-7.

3. Aini NS, Kharisma VD, Widyananda MH, Murtadlo AA, Probojati RT, Turista DD, *et al*. In Silico Screening of Bioactive Compounds from *Syzygium cumini* L. and *Moringa oleifera* L. Against SARS-CoV-2 *via* Tetra Inhibitors. Pharmacogn J. 2022;14(4):267-72.

4. Fahmi M, Kharisma VD, Ansori ANM, Ito M. Retrieval and Investigation of Data on SARS-CoV-2 and COVID-19 Using Bioinformatics Approach. Adv Exp Med Biol. 2021;1318:839-57.

5. Hui DS, Azhar EI, Madani TA, Ntoumi F, Rock R, Dar O, *et al*. The Continuing 2019-nCoV Epidemic Threat of Novel Coronaviruses to Global Health-The Lastest 2019 Novel Coronaviruses Outbreak in Wuhan, China. Int J Infect Dis. 2020;91(1):264-6.

6. Hosseini ES, Kashani NR, Nikzad H, Azadbakht J, Bafrani HH, Kashani HH. The novel coronavirus Disease-2019 (COVID-19): Mechanism of action, detection and recent therapeutic strategies. Virology. 2020;551:1-9.

7. Wijaya RM, Hafidzhah MA, Kharisma VD, Ansori ANM, Parikesit AP. COVID-19 In Silico Drug with Zingiber officinale Natural Product Compound Library Targeting the Mpro Protein. Makara J Sci. 2021;25(3):5.

8. Hartono, Suryawati B, Sari Y, Avicena A, Maryani, Sukmagautama C, *et al*. The effect of curcumin and virgin coconut oil towards cytokines levels in COVID-19 patients at Universitas Sebelas Maret Hospital, Surakarta, Indonesia. Pharmacogn J. 2022;14(1):216-25.

9. Kharisma VD, Ansori ANM, Jakhmola V, Rizky WC, Widyananda MH, Probojati RT, *et al*. Multi-strain human papillomavirus (HPV) vaccine innovation via computational study: A mini review. Res J Pharm Technol. 2022;15(8).

10. Kharisma VD, Ansori AN, Probojati RT, Turista DD, Antonius Y. Concept of SARS-CoV-2 Vaccine Design to Fight COVID-19 Pandemic: A Review Insight. Indian J Forensic Med Toxicol. 2021;15(4):2797-803.

11. Aini NS, Kharisma VD, Widyananda MH, Murtadlo AA, Probojati RT, Turista DD, *et al*. In Silico Screening of Bioactive Compounds from *Syzygium cumini* L. and *Moringa oleifera* L. Against SARS-CoV-2 via Tetra Inhibitors. Pharmacogn J. 2022;14(4):267-72.

12. Tacharina MR, Ansori ANM, Plumeriastuti H, Kusnoto , Kurnijasanti R, Hestianah EP. Beneficial effect of grinting grass (Cynodon dactylon) on the streptozotocin induced diabetes mellitus in the mice. Indian Vet J. 2020; 97(4): 35-38.

13. Kharisma VD, Agatha A, Ansori ANM, Widyananda MH, Rizky WC, Dings TGA, *et al*. Herbal combination from *Moringa oleifera* Lam. and *Curcuma longa* L. as SARS-CoV-2 antiviral via dual inhibitor pathway: A viroinformatics approach. J Pharm Pharmacogn Res. 2022;10(1):138-46.

14. Wahyuni DK, Ansori ANM, Vidiyanti F. GC-MS analysis of phytocomponents in methanolic extracts of leaf-derived callus of Justicia gendarussa Burm.f. Biosci Res. 2017;14(3):668-677.

15. Biswas D, Nandy S, Mukherhee A, Pandey DK, Dey A. *Moringa oleifera* Lam. and Derived Phytochemicals Are Promising Antiviral Agents: A Review. South Afr J Botany. 2020;129:271-82.

16. Hamza M, Ali A, Khan S, Ahmed S, Attique Z, UrRehman S, *et al*. Mass Fingerprinting Identification, Binding, and Blocking of Inhibitors Flavonoids and Anthraquinone of Moringa oleifera and Hydroxychloroquine. J Biomol Struct Dyn. 2021;39(11):4089-99.

17. Sharma P, Vijayan V, Pant P, Sharma M, Vikram N, Kaur P, *et al*. Identification of potential drug candidates to combat COVID-19: a structural study using the main protease (mpro) of SARS-CoV-2. J Biomol Struct Dyn. 2021;39(17):6649-59.

18. Aini NS, Kharisma VD, Widyananda MH, Murtadlo AA, Probojati RT, Turista DD, *et al*. Bioactive Compounds from Purslane (*Portulaca oleracea* L.) and Star Anise (Illicium verum Hook) as SARS-CoV-2 Antiviral Agent via Dual Inhibitor Mechanism: In Silico Approach. Pharmacogn J. 2022;14(4):352-7.

19. Ansori ANM, Kharisma VD, Solikhah TI. Medicinal properties of Muntingia calabura L.: A Review. Res J Pharm Technol. 2021;14(8):4509-2.

20. Mawaddani N, Wibowo NRK, Nadhira Q, Pramifta RA. In silico Study of Centella asiatica Active Compound as BACE1 Inhibitor in Alzheimer's Disease. J Smart Bioprosp Technol. 2020;1(2):37.

21. Ardiana R, Khasanah DU, Permatasari D, Adianingsih OR. Molecular Docking Study of Active Compounds in Amaranthus tricolor Leaves as High Mobility Group Box 1(HMGB1) Inhibitor in Breast Cancer. JSMAR Tech. 2020;2(1):28-34.

22. Kharisma VD, Kharisma SD, Ansori ANM, Kurniawan HP, Witaningrum AM, Fadholly A, *et al*. Antiretroviral Effect Simulation from Black Tea (Camellia sinensis) via Dual Inhibitors Mechanism in HIV-1 and its Social Perspective in Indonesia. Res J Pharm Technol. 2021;14(1):455-60.

23. Dibha AF, Wahyuningsih S, Ansori AN, Kharisma VD, Widyananda MH, Parikesit AA, *et al*. Utilization of Secondary Metabolites in Algae Kappaphycus alvarezii as a Breast Cancer Drug with a Computational Method. Pharmacogn J. 2022;14(3):536-43.

24. Widyananda MH, Pratama SK, Samoedra RS, Sari FN, Kharisma VD, Ansori ANM, *et al*. Molecular docking study of sea urchin (Arbacia lixula) peptides as multi-target inhibitor for non-small cell lung cancer (NSCLC) associated proteins. J Pharm Pharmacogn Res. 2021;9(4):484-96.

25. Proboningrat A, Kharisma VD, Ansori ANM, Rahmawati R, Fadholly A, Posa GAV, *et al*. In silico Study of Natural inhibitors for Human papillomavirus-18 E6 protein. Res J Pharm Technol. 2022;15(3):1251-6.

26. Antonius Y, Utomo DH, Widodo. Identification of potential biomarkers in nasopharyngeal carcinoma based on protein interaction analysis. Int J Bioinform Res Appl. 2017;13(4):376.

27. Ansori ANM, Kharsima VD, Muttaqin SS, Antonius Y, Parikest AA. Genetic variant of SARS-CoV-2 isolates in Indonesia: Spike glycoprotein gene. J Pure Appl Microbiol. 2020;14(Suppl 1):971-8.

28. Kuriata A, Gierut AM, Oleniecki T, Ciemny MP, Kolinski A, Kurcinski M, *et al*. CABS-flex 2.0: a web server for fast simulations of flexibility of protein structures. Nuc Acids Res. 2018;46(W1):W338-43.

29. Kharisma VD, Ansori ANM. Construction of Epitope-Based Peptide Vaccine Against SARS-CoV-2: Immunoinformatics Study. J Pure Appl Microbiol. 2020;14(suppl 1):999-1005.

30. Padmi H, Kharisma VD, Ansori ANM, Sibero MT, Widyananda MH, Ullah ME, *et al*. Macroalgae bioactive compounds for the potential antiviral of SARS-CoV-2: An in silico study. J Pure Appl Microbiol. 2022;16(2):1018-27.

31. Kharisma VD, Probojati RT, Murtadlo AAA, Ansori ANM, Antonius Y, Tamam MB. Revealing potency of bioactive compounds as inhibitor of dengue virus (DENV) NS2b/NS3 protease from sweet potato (Ipomoea batatas L.) leaves. Indian J Forensic Med Toxicol. 2021;15(1):1627-32.

32. Nguyen HL, Thai NQ, Truong DT, Li MS. Remdesivir Strongly Binds to Both RNA-Dependent RNA Polymerase and Main Protease of SARS-CoV-2: Evidence from Molecular Simulations. J Phys Chem B. 2020;124(50):11337-48.

33. Kavitha K, Sivakumar S, Ramesh B. 1,2,4 triazolo[1,5-a] pyrimidin-7-ones as novel SARS-CoV-2 Main protease inhibitors: In silico screening and molecular dynamics simulation of potential COVID-19 drug candidates. Biophys Chem. 2020;267:106478.

34. Mengist HM, Dilnessa T, Jin T. Structural Basis of Potential Inhibitors Targeting SARS-CoV-2 Main Protease. Front Chem. 2021;9(622898):4.

35. Hafidzhah MA, Wijaya RM, Probojati RT, Kharisma VD, Ansori ANM, Parikesit AA. Potential vaccine targets for COVID-19 and phylogenetic analysis based on the nucleocapsid phosphoprotein of Indonesian SARS-CoV-2 isolates. Indones J Pharm. 2021;3(3):328-37.

36. Kharisma VD, Ansori ANM, Dian FA, Rizky WC, Dings TGA, Zainul R, *et al*. Molecular docking and dynamics simulation of entry inhibitor from Tamarindus indica bioactive compounds against SARS-CoV-2 infection via viroinformatics study. Biochem Cell Arch. 2021;21(2):3323-7.

37. Turista DDR, Islamy A, Kharisma VD, Ansori ANM. Distribution of COVID-19 and Phylogenetic Tree Construction of SARS-CoV-2 in Indonesia. J Pure Appl Microbiol. 2020;14(suppl 1):1035-42.

38. Listiyani P, Kharisma VD, Ansori ANM, Widyananda MH, Probojati RT, Murtadlo AAA, *et al*. In silico phytochemical compounds screening of Allium sativum targeting the Mpro of SARS-CoV-2. Pharmacogn J. 2022;14(3):604-9.

39. Wang M, Cao R, Zhang L, Yang X, Liu J, Xu M, *et al*. Remdesivir and chloroquine effectively inhibit the recently emerged novel coronavirus (2019-nCoV) in vitro. Cell Res. 2020;30(3):269-71.

40. Warren TK, Jordan R, Lo MK, Ray AS, Mackman RL, Soloveva V, *et al*. Therapeutic efficacy of the small molecule GS-5734 against Ebola virus in rhesus monkeys. Nature. 2016;531(7594):381-5.

41. Mir SA, Firoz A, Alaidarous M, Alshehri B, Bin DAA, Banawas S, *et al*. Identification of SARS-CoV-2 RNA-dependent RNA polymerase inhibitors from the major phytochemicals of Nigella sativa: An in silico approach. Saudi J Biol Sci. 2021;29(1):394-401.

42. Aini NS, Kharisma VD, Widyananda MH, Murtadlo AA, Probojati RT, Turista DD, *et al*. Bioactive Compounds from Purslane (Portulaca oleracea L.) and Star Anise (Illicium verum Hook) as SARS-CoV-2 Antiviral Agent via Dual Inhibitor Mechanism: In Silico Approach. Pharmacogn J. 2022;14(4):352-7.

43. Padhi AK, Shukla R, Saudagar P, Tripathi T. High-throughput rational design of the remdesivir binding site in the RdRp of SARS-CoV-2: implications for potential resistance. Science. 2020;24(1):101992.

44. Vyshnava SS, Pandluru G, Kumar KD, Panjala SP, Paramasivam K, Banapuram S, *et al*. A Computational Approach for Protein-Protein Interactions of Bacterial Surface Layer Protein with Human Erb3 and αIIB-β3 Receptors. Biointerface Res Appl Chem. 2020;12(1):420-30.

45. Ansori ANM, Antonius Y. A phylogenetic analysis of Indonesian SARS-CoV-2 isolates from March to December 2020: Compared with Delta and Mu variant. J Teknologi Laboratorium. 2022;11(1).

46. Mishra A, Rathore AS. RNA dependent RNA polymerase (RdRp) as a drug target for SARS-CoV2. J Biomol Struct Dyn. 2020;40(13):4041-6047.

47. Agahi F, Juan C, Font G, Juan-García A. In silico methods for metabolomic and toxicity prediction of zearalenone, α-zearalenone and β-zearalenone. Food Chem Toxicol. 2020;146:111818.

48. Ongko J, Setiawan JV, Feronytha AG, Juliana A, Effraim A, Wahjudi M, *et al*. In-silico screening of inhibitor on protein epidermal growth factor receptor (EGFR). IOP Confe Series: Earth Env Sci. 2022;1041:012075.

49. Jin Z, Du X, Xu Y, Deng Y, Liu M, Zhao Y, *et al*. Structure of M Pro from SARS-CoV-2 and Discovery of Its Inhibitors. Nature. 2020;582(7811):289-93.

50. Kumar S, Gupta S, Gaikwad S, Abadi LF, Bhutani LKK, Kulkarni S, *et al*. Design, Synthesis and in Vitro Evaluation of Novel Anti-HIV 3-Pyrazol-3- yl-Pyridin-2-One Analogs. Med Chem. 2019;15(5):561-70.

GRAPHICAL ABSTRACT

Moringa oleifera

SARS-CoV-2

ABOUT AUTHORS

Rahadian Zainul has completed a Bachelor of Educational Chemistry in IKIP Padang, then continued his studies and obtained a Master of Chemistry at Universitas Andalas, and earned a Doctoral Chemistry degree at Universitas Andalas. He is a researcher on the design and modification of copper oxide for inactivation SARS-CoV-2 by stimulated indoor lights and a researcher on the design and modification of copper oxide by computation approach with DFTB+. He is also the Head of Cambiotics Research Center, Universitas Negeri Padang. The author has published 41 manuscripts in Scopus-indexed journals and also 8 h-index.